DOI: 10.1002/ejic.200800463

H-Bonded Porous Supramolecular Network of a Cu^{II} Complex Assisted by Assembled 2D Sheet of Chair Form Hexameric Water Cluster

Kafeel Ahmad Siddiqui,[a] Gopal K. Mehrotra,*[a] Jerzy Mrozinski,[b] and Raymond J. Butcher[c]

Keywords: Transmetallation / Copper complex / Hydrogen bonds / Porous supramolecular network

The supramolecular network of the complex having the formula $[Cu(nicot)_2{\cdot}2NH_3{\cdot}2H_2O]{\cdot}6H_2O$ **1** has been synthesized by transmetallation of the Zn–nicotinate complex by Cu^{II} ions and its crystallization in an ionic liquid. The supramolecular network of **1** shows unique H-bonding in the sense that it not only participates in the formation of nanoporous 2D chains but also forms cyclic hexameric water cluster that adopt an ice-like chair conformation, which together with octanuclear H-bonded rings extend the network into a 3D open framework. X-ray structural analysis, FTIR, thermal analysis, EPR and magnetic properties have been used to characterize this compound.

Introduction

Pronounced interest has recently been focused on the synthesis and characterizations of H-bonded supramolecular materials which offer themselves as attractive molecular models connecting molecular to supramolecular chemistry. Due to the reversible nature of the intermolecular interactions and relatively poor stability, these structures seem to have dynamic properties not found in covalent bonded coordination polymers. It is known that in aqueous solution aggregates of water molecules $(H_2O)_n$ clusters help stabilize both natural and synthetic supramolecular species. In this relevance, self-assembled H-bonded water clusters found trapped in a crystal host are of particular interest because of their unusual properties and vital role played by them in many physical, chemical and biological processes.[1,2] A number of small water clusters in diverse surroundings have been widely investigated both from theoretical and experimental aspects in order to better understand anomalous nature of bulk water or ice I_h[1] These H-bonded water clusters of different morphologies such as tetramers, pentamers, hexamers, heptamers, octamers and decamers or polymeric chains, tape or layer structures have been found trapped in organic molecular crystals as well as in metal-organic frameworks.[3,4,5] Of these, the water hexamer, a simple supramolecular analogue of cyclohexane, is of particular interest in the sense that beside existing in different isoenergic isomeric forms it also exhibits some of the properties found in bulk water.[6,7,8] Hexameric water also forms a liquid crystalline lattice that is involved in cellular communication, intracellular water movement, enzyme function and many other metabolic processes. In addition to the above-mentioned fundamental importance, the H-bonded aggregates have been reported to possess interesting magnetic properties.[4a,5b]

In this context, we have noticed that in order to strategically design and synthesize metal-organic framework (MOF) structures where metal complexes act as binder for small water clusters, most of the workers have so far adopted the route of one-pot synthesis.[3,4,5] To date there is no report on the synthesis of porous supramolecular network of a metal complex formed by transmetallation. Here we describe the preparation, crystal structure and magnetic studies of a 3D porous supramolecular network of the complex $[Cu(nicot)_2{\cdot}2NH_3{\cdot}2H_2O]{\cdot}6H_2O$ (**1**) formed by transmetallation of Zn–nicotinate complex by Cu^{II} ion and its crystallization in an ionic liquid (25% ammonia solution) that is stabilized by an intricate array of H-bonded interactions involving contributions from solvent water clusters, namely a water hexamer $[(H_2O)_6]$ with ice-like molecular arrangement.

Results and Discussion

Description of the Supramolecular Network

The synthesis of the complex **1** is shown in Scheme 1.

---

[a] Department of Chemistry, M. N. National Institute of Technology Allahabad,
211004, U.P., India
E-mail: gkmehrotra@mnnit.ac.in
[b] Faculty of Chemistry, Wroclaw University,
F. Joliot-Curie 14 Street, 50-383 Wroclaw, Poland
[c] Department of Chemistry, Howard University,
Washington, DC 20059, USA

Supporting information for this article is available on the WWW under http://www.eurjic.org or from the author.

$$Zn^{II} + \text{nicotinic acid} \longrightarrow [Zn(nicot)_2{\cdot}4H_2O]\ \text{(white)}$$

$$[Zn(nicot)_2{\cdot}4H_2O] + Cu^{II} \longrightarrow [Cu(nicot)_2{\cdot}4H_2O]\ \text{(sky blue)}$$

$$[Cu(nicot)_2{\cdot}4H_2O] \xrightarrow{\text{25\% ammonia}} [Cu(nicot)_2{\cdot}2NH_3{\cdot}2H_2O]{\cdot}6H_2O]\ \mathbf{1}\ \text{(deep blue)}$$

Scheme 1. Synthetic steps involved in **1**.

The asymmetric unit of triclinic crystal lattice with $P\bar{1}$ (space group number 2) contains one crystallographically independent Cu^{II} ion to which two nicotinate ions are coordinated axially through N atoms, whereas two water molecules and two ammonia molecules complete the octahedral coordination sphere. The coordination of nitrogen atoms of each nicotinate ions and ammonia molecules results in the formation of two symmetrical axis N···Cu···N1A, N2···Cu···N2A respectively. The oxygen atoms of water molecules describe the third axis O1w···Cu···O1wA (S1). The Cu···N distance for both ammonia (Cu···N2 2.0192 Å) and nicotinate ion (Cu···N1 2.0621 Å) is shorter than the Cu···O distance of coordinated water (Cu···O1w 2.524 Å). The Cu···N bond lengths listed in Table 1S (Supporting Information) which lies in the normal range similar to distorted octahedral Cu^{II} complexes.

In order to interpret the whole network clearly, separate description of each unit is needed. The units of copper nicotinate complex are oriented in such a way that supramolecular $\{[Cu(nicot)_2{\cdot}2NH_3{\cdot}2H_2O]{\cdot}6H_2O\}_n$ chains are generated through point reflection at crystallographic inversion centers (see parts a and b in Figure 1). These polymeric chains are held together by pairs of hydrogen bond. Four (two O4w, two O2w) water molecules of crystal lattice together with coordinated water molecules are interconnected with crystallographically same copper complex units forms cyclic hexameric water cluster that adopts an ice like chair conformation (Figure 2, a), propagating the formation of H-bonded one dimensional chains (Figure 2, b), which is further connected by remaining two water molecules (O3w) of crystal lattice to form 3D extended supramolecular network having a separation distance of 4.792 Å (Figure 2, c). A closer examination of the packing reveals the extended nanometer channels, approximately 8.75 Å × 11.32 Å wide (based on Cu···Cu distance) through the crystal. Their existence seems to originate in the highly asymmetric shape of the hydrogen bonded building block, which precludes efficient packing of layers. The carboxylato ion of the nicotinic acid of the complex is *anti* with respect to copper atom. The oxygen atom of carboxylate ion of nicotinic acid of two units together with the independent water molecules (two O2w, two O4w, and two O3w) present in the crystal lattice built a hydrogen bonded octanuclear ring with a diameter of 6.366 Å (Figure 3.). The octanuclear rings are interconnected by the hexameric water cluster through H-bonding on both the side by O2w, and O4w lattice water molecules results in the formation of 3D supramolecular network (Figure 4).

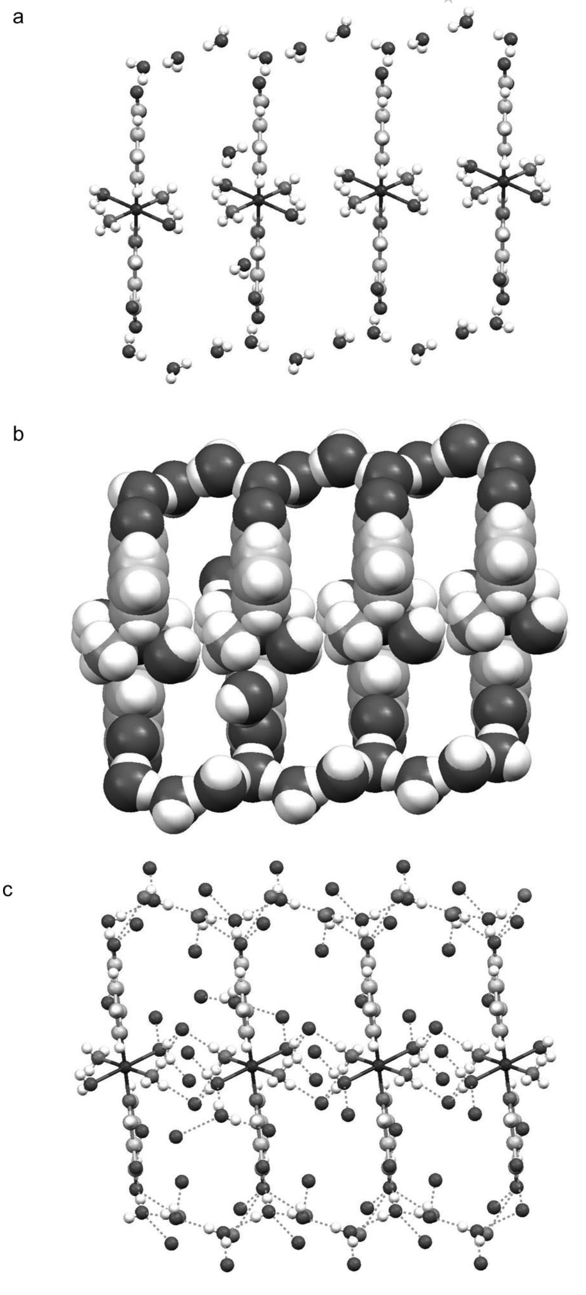

Figure 1. (a): Fragment of the crystal lattice showing the intercalation of parallely stacked supramolecular chains of copper complex; (b): space-filled diagram showing pores; c: perspective view showing the dimeric units and the H-bonding interactions in **1** (oxygen: dark grey, hydrogen: white, carbon: light grey, nitrogen: grey, copper: black).

The assembled hexameric water cluster identified in the supramolecular network is associated with the host framework by H-bonds in the channels of **1** (Table 1.) The hexamer is in close analogy with ice I_h, contains assembled hydrogen bonded hexameric rings, having an all chair conformation.[13] It is apparent that its configuration (*all-cis*) is different from the one found in ice I_h (*all-trans*), and is connected by two independent lattice water molecules in the

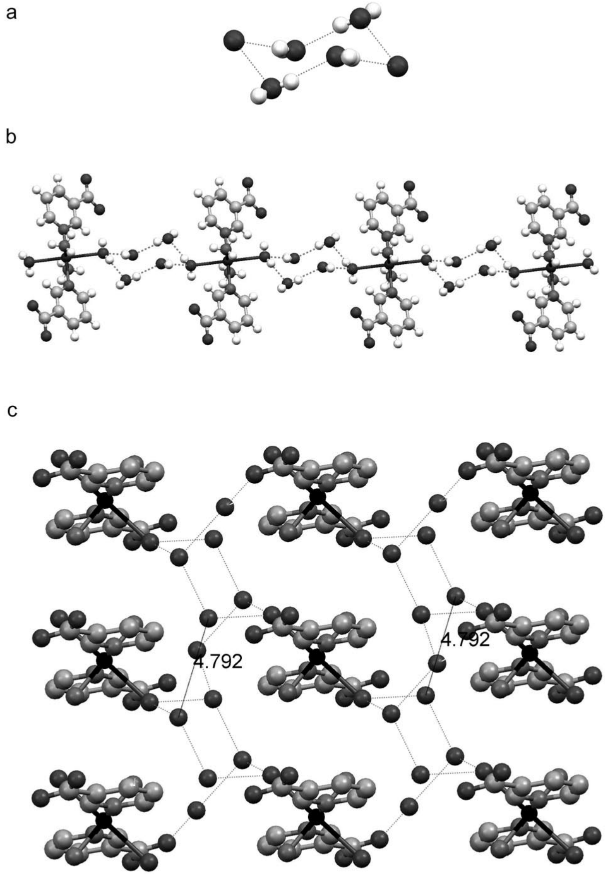

Figure 2. (a): Chair form water cluster; (b): chair form water cluster between the units of the complex forming the 2D linear chain; (c): intercalation of two linear chain by two lattice water molecules with a separation distance of 4.792 Å to form an overall 3D H-bonded supramolecular network (H atoms are omitted for clarity).

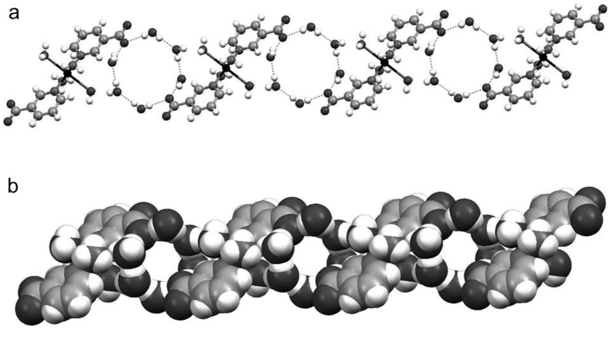

Figure 3. (a): A fragment of crystal lattice showing the intercalation of units of complex in head to tale fashion through H-bonding forming octanuclear cyclic ring; (b): space-filled diagram showing octanuclear rings having pores of diameter 6.366 Å.

nanometer channel 8.75 Å × 11.32 Å wide (based on Cu···Cu distances) to form assembled water hexamers, in which all water molecules are involved in hydrogen bond only, and which have a clearly defined hydrogen-bonding system.

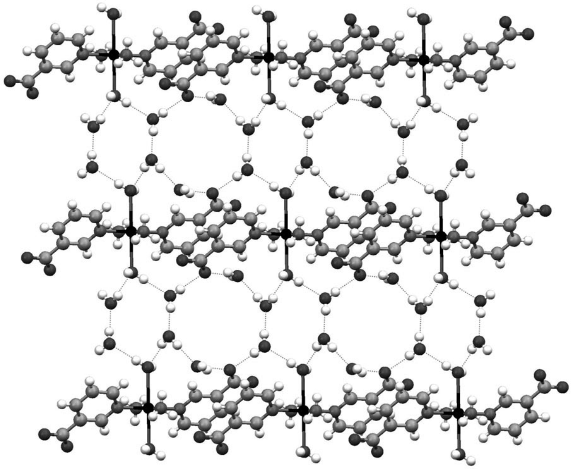

Figure 4. Chair form water cluster together with octanuclear H-bonded ring extend the H-bonded network into a 3D open framework.

The geometrical parameters of the H-bond in water hexamers and its association with host are summarized in the Table 1. The O···O distance in the hydrogen bonds found in this supramolecular structure of water hexamer range from 2.76 to 2.84 Å, within an average value of 2.80 Å. From comparison, the O···O separation in ice I_h (T = 60 K) and liquid water are 2.75 and 2.85 Å, respectively.[8,14] The average O···O distance of 2.80 Å is smaller than that of liquid water which shows a value of 2.85 Å from the X-ray diffraction radial distribution curve while for the gas phase, this value is about 0.1 Å longer.[15,16] The interhexamer O(3)···O(2) and O(3)···O(4) distance is 2.827 Å and 2.758 Å, respectively, which is also very similar to the O···O distance of liquid and water ice I_h. The water molecules present in cleft of biological/abiological molecules are very different from the gas phase or bulk liquid water. Here, the principle of maximizing H-bonding interaction is followed where the host environment plays a major role. Consistent with this principle, the O···O distance in the cluster vary widely for optimized interactions between the water molecules and its surrounding. However, there is a wide variation in the O···O···O angles, with an average value of 114.9°. This value deviates considerably from the corresponding value of 109.3° in hexagonal ice.

The non-bonding O···O···O angles (Table 2) of **1** span a wide range (from 94° to 118°) deviating considerably from an ideal chair form cyclohexane structure. In the chair form water hexamer, both O2w act as double donor and double acceptor showing [2+2] H-bonding pattern, thus oxygen atom have "formal" coordination numbers of four (two hydrogen atoms acts as accepter, and two lone pairs as donor) with approximately tetrahedral arrangement. O4w act as double acceptor and a sole donor which is connected to the coordinated water molecule of the host framework through O4–H···Ow1 hydrogen bonding. While the O3w also act as donor and double acceptor of H-bonding and is coordi-

Table 1. Hydrogen bonds for **1** [Å, °].

D–H···A	*d*(D–H)	*d*(H···A)	*d*(D···A)	<(DHA)
O(1w)–H(1w1)···O(2w)#2	0.832(14)	1.973(15)	2.7854(14)	165.0(17)
O(1w)–H(1w2)···O(2)#3	0.817(16)	1.958(16)	2.7693(12)	172(2)
O(2w)–H(2w1)···O(1)	0.765(15)	1.965(15)	2.7280(13)	175(2)
O(2w)–H(2w2)···O(4w)#4	0.792(16)	1.989(16)	2.7717(14)	170(2)
O(3w)–H(3w1)···O(1)	0.761(16)	2.035(16)	2.7648(13)	161(2)
O(3w)–H(3w2)···O(2w)#5	0.754(16)	2.098(18)	2.8270(14)	163(3)
O(4w)–H(4w1)···O(1w)	0.794(16)	2.058(17)	2.8428(14)	170(3)
O(4w)–H(4w2)···O(3w)#1	0.824(16)	1.936(17)	2.7578(15)	175(3)
N(2)–H(2N1)···O(4w)#6	0.860(14)	2.531(16)	3.2409(14)	140.5(15)
N(2)–H(2N3)···O(2)#2	0.861(14)	2.148(14)	3.0024(13)	171.3(16)
N(2)–H(2N2)···O(2)#3	0.867(14)	2.259(15)	3.0595(13)	153.5(16)

Symmetry transformations used to generate equivalent atoms (D = donor, A = acceptor): #1: –*x*, –*y* + 1, –*z*; #2: –*x* + 1, –*y* + 1, –*z* + 1; #3: *x*, *y*, *z* – 1; #4: *x*, *y* – 1, *z* + 1; #5: –*x* + 1, –*y*, –*z* + 1; #6: *x*, *y* – 1, *z*.

nated to O1 of carboxylate oxygen of nicotinate ion through O3w···O1 hydrogen bonding and water molecule of hexamers through O3w···H–O4w hydrogen bonds. So, every O atom in the unit does not show four coordination. Such hydrogen-bond deficient water molecules are present at the surface of ice[17] while recent X-ray absorption spectroscopy and Raman scattering studies of liquid water also point to the fact that significant number of O atoms show less than tetra-coordination in liquid water.[18]

Table 2. The geometrical parameter of the H-bond in water hexamer [Å, °].

O1w–H···O2w	164.76	O1w···O2w···O4w	112.58
O2w–H···O4w	170.06	O1w···O4w···O2w	110.96
O4w–H···O1w	169.78	O3w···O4w···O1w	94.19
O1w···O2w	2.785	O3w···O4w···O2w	138.89
O1w···O4w	2.843	O2w···O3w···O1	121.61
O2w···O4w	2.772	O4w···O3w···O1	104.21
O2w···O3w	2.827		
O4w···O3w	2.758		
O3w···O1	2.765		

Notably, there are no Ow–H···N or NH···Ow hydrogen bonds between the water cluster and coordinated ammonia molecules but O1···H–Ow hydrogen bonding is present between lattice water molecule and nicotinate ion that forms an octanuclear cyclic ring of the pore diameter of about 6.366 Å. This structure appears, therefore, to be unique in the sense that to some extent the water molecules in the cluster experience a molecular surrounding that resemble more closely to the environment found in liquid water or ice as opposed to the previously described inclusion complexes of water clusters in which strong interactions with the host are present.[3,19]

Since H-bonding and porosity plays important role in chemistry and biology, a detailed structural knowledge of such types of porous metallo-supramolecular networks might contribute in better understanding some natural biochemical and pharmacological processes.[7,20,21]

Magnetic and EPR Properties

Variable-temperature magnetic susceptibility data were collected for a powdered sample in the temperature range from 1.8 to 300 K. The temperature variation of magnetic susceptibility (χ_M) and $\chi_M T$ of as synthesized complex is illustrated (Figure 5, a) by means of a plot of χ_M (M = Cu) vs. the temperature, the values of $\chi_M T$ are slightly dependent of the temperature. At 300 K, the $\chi_M T$ value is 0.43 cm^3 mol^{-1} K as expected to two magnetically isolated copper ions.[22] Upon cooling from room temperature the $\chi_M T$ value remains almost constant till 50 K and then sharply decreases to 0.32 cm^3 mol^{-1} K as the temperature is lowered to 1.8 K.

The effective magnetic moment μ_{eff}, per Cu^{II} lowering from 1.84 at 300 K to 1.63 at 1.8 K, which confirms the magnetic moments for mononuclear Cu^{II} complex,[23] together with the negative Weiss (θ) = –1.4 K constant. A negative Weiss constant value for the complex can suggests a very weak intermolecular antiferromagnetic interactions occurring in the crystal lattice of complex and is consistent with the single crystal data where the two Cu^{II} centers are far apart (Cu–Cu distance 10.923 Å) and are not directly bridged by ligand atoms clearly indicating that the supramolecular network of **1** is a consequence of non covalent interaction (H-bonding). It can be assumed that the hydrogen-bonded water groups (hexameric water cluster) provide important exchange pathways between two Cu^{II} centre (Figure 2, b), probably by means of spin polarization mechanism.[4a] Weiss constant was calculated for temperature range form 100 to 300 K, because small anomalies for the $\chi_M^{-1} = f(T)$ relation were observed in the lowest temperature range only (Figure 5, b). Hence, the experimental data between from 1.8 to 50 K have been fitted to the molecular field correction. The best fitting parameter obtained is $zJ' = -0.57$ cm^{-1} as a result minimizing the function *R* to 1.29×10^{-4}.

The magnetization vs. magnetic field curve for complex at 2 K (Figure 5, c) increases and indicates value of the magnetization 0.92 B.M. at 5 Tesla, which confirms the ground state of the complex with $S = ½$ and $g \approx 2$.

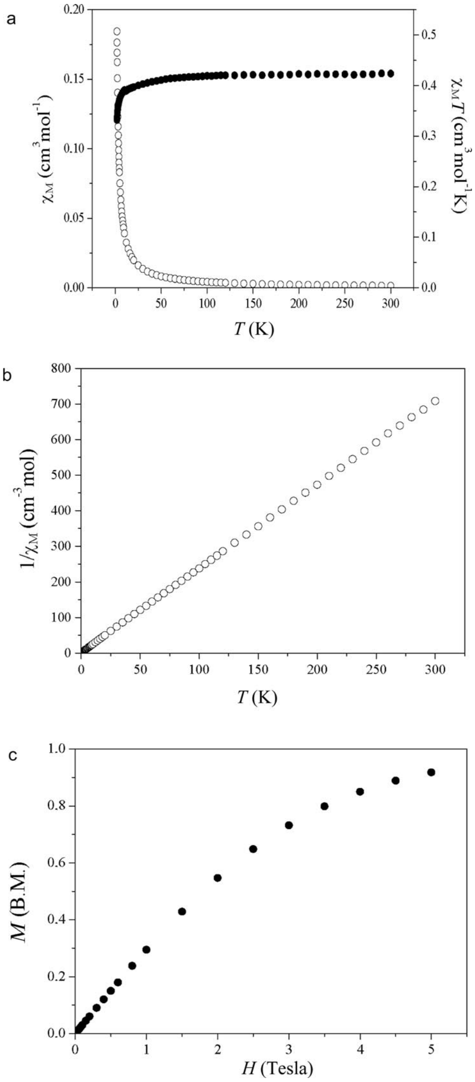

Figure 5. (a): Plot of (χ_M, M = Cu) χ_{Cu} (o) and χ_{Cu} T (•) vs. T for **1**. The solid line is the results of the best fit obtained with the parameters reported in the text; (b): plot of the 1/χ_m vs. T for the complex; (c): the variation of the magnetization M vs. magnetic field H for complex at 2 K.

$$\chi_M = \frac{N\beta^2 g_{av}^2}{3kT} s(s+1)$$

$$\chi_M^{\mathrm{corr}} = \frac{\chi_M}{1 - \dfrac{2zJ'\,\chi_M}{Ng_{av}^2\,\beta^2}}$$

where $$R = \sqrt{\frac{\sum_{i=1}^{n}\left[(\chi_M^{\exp})_i - (\chi_M^{calc})_i\right]^2/(\chi_M^{\exp})_i^2}{\sum_{i=1}^{n} 1/(\chi_M^{\exp})_i^2}}$$

The X-band solid state EPR spectrum (Figure 6) of **1** does not change with temperature (from 273 K to 77 K). It shows typical axial pattern[24] with $g_{\parallel}$ = 2.25, $g_{\perp}$ = 2.06 corresponding to the $d_{x^2-y^2}$ ground state.

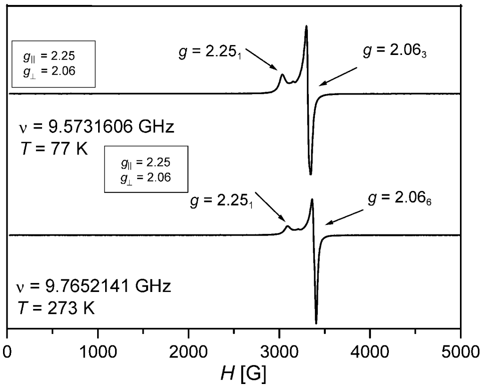

Figure 6. EPR spectra of complex **1** at 77 K and 273 K.

Thermal Analysis

The 3D structure is largely a consequence of hydrogen bonding interactions among water molecules themselves and the MOF. This association is quite strong as thermal gravimetric analysis (Figure 2S, Supporting Information) of **1** with a 5.62 mg sample in N_2 shows that the compound begins to lose weight above 60 °C. Water removal begins at 80 °C and the loss of all the water molecules takes place at 115 °C. The loss of coordinated ammonia occurs at 151 °C. The complete decomposition of the compound is achieved above 255 °C. DTA analysis of crystal showed three endothermic peaks at 115 °C, 151 °C and 255 °C, which is attributed to the release of coordinated water, ammonia and nicotinate ion from the copper ion respectively.

The FTIR spectrum (Figure 3S) of the as synthesized complex shows a broad band centered around 3376 cm^{-1} which vanishes on heating the compound under vacuum (0.1 mm) at 120 °C for 2 hours due to escape of water from the lattice. While a short peak at 3432 cm^{-1} is due to the O–H frequency of the coordinated water. Deliberate exposure to water vapour for 2 days do not lead to re-absorption of water into lattice as monitored by FTIR spectroscopy. The O–H stretching vibration of small water clusters $(H_2O)_n$ (n = 2 to 10) in the gaseous state have been investigated using infrared depletion fragment spectroscopy. The stretching vibrations are found to be size specific spreading over a wide range from 3720 to 2935 cm^{-1} with the vibration below 3400 cm^{-1}. In comparison, the O–H stretching vibration in ice appears at 3220 cm^{-1} while in liquid it shifts to 3280 to 3490 cm^{-1}.[2b] Therefore, the O–H stretching frequency of the water cluster in **1** is more like liquid water with a slight variation attributed to its surrounding. This result is expected, as the water cluster acts as a "glue" to assemble the supramolecular network around it leading to the 3D structure (Figure 2, c).

Conclusions

In summary, a new H-bonded porous supramolecular network of the metal complex $[Cu(nicot)_2{\cdot}2NH_3{\cdot}2H_2O]{\cdot}6H_2O$ (**1**) has been synthesized and characterized structurally and magnetically. The X-ray analysis of the complex **1** has revealed a three-dimensional structure which is stabilized by H-bonded water clusters. Thermogravimetric and FTIR study clearly indicate that the water cluster acts as a "stick" to assemble the supramolecular network around it leading to the 3D structure. The magnetic susceptibility measured over the range of 1.8 to 300 K shows very small negative value of θ in the complex suggesting the existence of a very weak intermolecular antiferromagnetic exchange between copper ions within the crystal lattice via the H-bonded system. Thus, this study will largely enrich the field of metallo-supramolecular chemistry and understanding of the nature and extent of H-bonding in such materials. This synthetic strategy will also open a new gateway for the preparation of supramolecular assembly via transmetallation in ionic liquids.

Experimental Section

Materials and Methods: All chemicals of reagent grade were commercially available and used without further purification. The infrared spectrum of KBr pellets in the form 4000 to 500 cm^{-1} was recorded with a FTIR spectrometer (KBr pellets). Thermal analysis (TG-DTA) was carried out with a Setsys TG-DTA 16 instrument. X-ray powder diffraction was performed with a CCD area detector diffractometer, equipped with a graphite monochromator and Mo-K_α radiation (λ = 0.71073 Å). Magnetization measurements of polycrystalline samples were carried out with a Quantum Design SQUID magnetometer (MPMSXL-5-type) at a magnetic field of 0.5 Tesla over the temperature range 1.8–300 K. EPR spectra were recorded at room temperature and 77 K on a Bruker ESP 300 spectrometer operating at X-band equipped with an ER 035M Bruker NMR gaussmeter and HP 3530B Hewlett–Packard microwave frequency counter.

Crystallography: A single-crystal of **1** (size $0.47 \times 0.23 \times 0.18$ mm^3) was mounted on a CCD area detector diffractometer, equipped with a graphite monochromator and Mo-K_α radiation (λ = 0.71073 Å). The unit cell dimensions and intensity data were measured at 200(2) K. The structure was solved by direct methods, and refined by the full-matrix least square based on F^2 with anisotropic thermal parameters for the non-hydrogen atoms using Bruker, SMART (data collection and cell refinement), Bruker SAINT (data reduction) SHELX-97 (structure solution), and SHELXL-97 (structure refinement) and Bruker SHELXTL (molecular graphics).[9–12]A multi-scan adsorption correction (SADABS) was applied. The experimental XRD patterns agreed well with the simulated ones generated on the basis of single-crystal analysis of the complex, suggesting the phase purity of the product. Hydrogen atoms were included in geometrically calculated positions using a riding model and were refined isotropically. Crystal data and structure refinement of complex are listed in Table 2S (Supporting Information).

CCDC-683978 contains the supplementary crystallographic data for this paper. These data can be obtained free of charge from The Cambridge Crystallographic Data Centre www.ccdc.cam.ac.uk/data_request/cif.

Synthesis: Nicotinic acid (0.64 g, 5.2 mmol) was dissolved in 70 cm^3 of hot water (80 °C) and then cooled to room temperature. The solution was added drop wise to an aqueous solution (10 mL) of $\mathrm{Zn(CH_3COO)_2{\cdot}2H_2O}$ (0.45 g, 2.6 mmol). The reaction mixture was stirred for about 10 min followed by the dropwise addition of *N*,*N*,*N'*,*N'*-tetramethylethylenediamine (TMED) (0.77 mL, 1 mmol), after that the whole reaction mixture was further stirred for about 30 min. The white crystalline material obtained was washed with distilled water and methanol and dried. The white powder was added to an aqueous solution (10 mL) of $\mathrm{CuCl_2{\cdot}2H_2O}$ (0.34 g, 2 mmol) with continuous stirring. The blue reaction mixture was stirred for 2 h and the resulting sky-blue precipitate was filtered, washed with distilled water and methanol and dried in air. The sky-blue powder was dissolved in 10 mL of 25% ammonia solution and left at room temperature for crystallization whereupon after 25 days fine deep blue needle-shaped crystals of **1** were obtained. IR (KBr): $\tilde{\nu}$ = 3376 (w), 1611 (s), 1571 (sh), 1393 (s), 1252 (s), 1194 (m), 1056 (s) cm^{-1}. $\mathrm{C_{12}H_{30}CuN_4O_{12}}$ (485.94): calcd. C 29.69, H 6.18, N 11.54; found C 29.68, H 5.98, N 11.49, yield 65%.

Supporting Information (see also the footnote on the first page of this article): Molecular structure of **1** (Figure 1S), thermogravimetric analysis (Figure 2S), FTIR spectra (Figure 3S), XRPD pattern of **1** (Figure 4S), bond lengths and angles (Table 1S), crystal and structure refinement data (Table 2S).

Acknowledgments

We acknowledge the support from theMotilal Nehru National Institute of Technology, Allahabad, India in the form of a research grant and award of institute's research fellowship to one of us (K. A. S.).

---

[1] a) K. Mitsuoka, K. Murata, T. Walz, T. Hirai, P. Agre, J. B. Heymann, A. Eagel, Y. Fujiyoshi, *J. Struct. Biol.* **1999**, *128*, 34–43; b) I. Ohmine, S. Satio, *Acc. Chem. Res.* **1999**, *32*, 741–748; c) U. Buck, F. Huisken, *Chem. Rev.* **2000**, *100*, 3863–3890; d) *Latest Developments in the Chemistry of Water Clusters* in Special Issue: K. V. Katti, P. K. Bharadwaj, J. J. Vittal, R. Kannan, *Synth. React. Met.-Org. Nano-Met. Chem.* **2008**, *38*, 1; e) M. H. Mir, J. J. Vittal, *Crystal Growth and Design*, **2008**, published online April/22/2008.

[2] a) R. Ludwig, *Angew. Chem. Int. Ed.* **2001**, *40*, 1808–1827; b) D. Eisenberg, W. Kauzmann, *The Structure and Properties of Water*, Oxford University Press, Oxford, **1969**; c) F. A. Quiocho, D. K. Wilson, N. K. Vyas, *Nature* **1989**, *340*, 404–407; d) J. Rosenthal, J. M. Hodgkiss, E. R. Young, D. G. Nocera, *J. Am. Chem. Soc.* **2006**, *128*, 10474–10483.

[3] a) B. Qing, H. L. Sun, S. Gao, *Angew. Chem. Int. Ed.* **2004**, *43*, 1374–1376; b) P. R. Cuamatzi, G. V. Diaz, H. Hopfli, *Angew. Chem. Int. Ed.* **2004**, *43*, 3041–3044; c) R. Custelcean, C. Afloroaei, M. Vlassa, M. Polverejan, *Angew. Chem. Int. Ed.* **2000**, *39*, 3094–3096; d) S. Pal, N. B. Sankaran, A. Samanta, *Angew. Chem. Int. Ed.* **2003**, *42*, 1741–1743; e) A. Mukherjee, M. K. Saha, M. Netaji, A. R. Chakravarty, *Chem. Commun.* **2004**, 716–717.

[4] a) K. V. Langenberg, S. R. Batten, K. J. Berry, D. C. R. Huckless, B. Moubaraki, K. S. Murray, *Inorg. Chem.* **1997**, *36*, 5006–5015; b) S. Monikumari, V. Shivaiah, S. K. Das, *Inorg. Chem.* **2002**, *41*, 6953–6955; c) J. L. Atwood, L. J. Barbour, T. J. Ness, C. L. Raston, P. L. Ratson, *J. Am. Chem. Soc.* **2001**, *123*, 7192–7193.

[5] a) S. K. Ghosh, P. K. Bharadwaj, *Inorg. Chem.* **2004**, *43*, 5180–5182; b) J. Qu, W. Gu, L. Z. Zhang, X. Liu, D. Z. Liao, *Inorg. Chem. Commun.* **2007**, *10*, 971–974.

[6] a) K. Liu, M. G. Brown, C. Carter, R. J. Saykally, J. K. Greorgy, D. C. Clary, *Nature* **1996**, *381*, 501–503; b) B. Zhao, P. Cheng, X. Y. Chen, C. Cheng, W. Shi, D. Z. Liao, S. P. Yan, Z. H. Jiang, *J. Am. Chem. Soc.* **2004**, *126*, 3012.

[7] a) P. J. Rosskey, *Nature* **2002**, *419*, 889–890; b) The relative stability of these isomers strongly depend on the temp. and zero

point (ZPE) correction, J. Kim, K. S. Kim, *J. Chem. Phys.* **1998**, *109*, 5886–5895.

[8] a) G. A. Jeffrey in *An Introduction to Hydrogen bonding*, Oxford University Press, New York, **1997**; b) J. N. Moorthy, R. Natarajan, P. Venugopalan, *Angew. Chem. Int. Ed.* **2002**, *41*, 3417; c) S. K. Ghosh, P. K. Bharadwaj, *Angew. Chem. Int. Ed.* **2004**, *43*, 3577.

[9] Bruker *SMART*, *SAINT*, and *XPREP*, AREA dectetor control and data integration and reduction software, Bruker Analytical X-ray Instruments Inc., Madison, WI, USA, **1995**.

[10] G. M. Sheldrick, *SADABS*, Program for the empirical absorption correction of area detector data, University of Göttingen, Germany, **1997**.

[11] G. M. Sheldrick, *Acta Crystallogr., Sect. A* **1990**, *46*, 467–473.

[12] G. M. Sheldrick, *SHELXL-97*, Programme for the refinement of crystal structure, University of Göttingen, Germany, **1997**.

[13] T. Dahl, *Acta Chem. Scand. Ser. B* **1987**, *41*, 379–382.

[14] W. F. Kuhs, M. S. Lehman, *J. Phys. Chem.* **1983**, *87*, 4312.

[15] D. Eisenberg, W. Kauzmann, *The Structure and Properties of Water*, Oxford University Press, **1969**.

[16] N. H. Fletcher, *The Chemical Physics of Ice*, Cambridge University Press, **1970**.

[17] a) C. J. Gruenloh, R. Corney, C. A. Arriangton, T. S. Zwiter, S. V. Fredrick, K. D. Jardon, *Science* **1997**, *276*, 1678; b) U. Buck, I. Ettischer, M. Melzer, V. Buch Sadlej, *J. Phys. Rev. Lett.* **1998**, *80*, 2578–2581.

[18] P. Warnet, D. Nordlund, U. Bergmann, M. Cavalleri, M. Odelius, H. Ogasawara, L. A. Naslund, T. K. Hirsch, L. Ojamae, P. Glatzel, L. G. M. Pettersson, A. Nilsson, *Science* **2004**, *304*, 995–999.

[19] a) W. B. Blanton, S. W. Gordon-Wylie, G. R. Clark, K. D. Jordon, J. T. Wood, U. Geiser, T. J. Collins, *J. Am. Chem. Soc.* **1999**, *121*, 3551–3552; b) L. J. Barbour, G. W. Orr, J. L. Atwood, *Nature* **1998**, *393*, 671–672; c) C. Foces-Foces, F. H. Cano, M. Martinez-Ripoll, R. Faure, C. Roussel, R. M. Claramunt, C. Lopez, D. Sanz, J. Elguero, *Tetrahedron: Asymmetry* **1990**, *1*, 65–86.

[20] L. J. Scatena, M. G. Brown, G. L. Richmond, *Science* **2001**, *292*, 908–912.

[21] S. Baldeli, C. Schintzer, D. J. Campbell, M. J. Schultz, *J. Phys. Chem. B* **1999**, *103*, 2789–2795.

[22] *SAINT*$^+$, rel. 6.02, Bruker AXS, Madison, WI **1999**.

[23] F. A. Cotton, G. Wilkinson, *Advanced Inorganic Chemistry*, 6th ed. Wiley, New York, **1999**, p. 867.

[24] B. J. Hathaway, D. E. Billing, *Coord. Chem. Rev.* **1970**, *5*, 143–207.

Received: May 8, 2008